We are IntechOpen, the world's leading publisher of Open Access books Built by scientists, for scientists

4,800
Open access books available

122,000
International authors and editors

135M
Downloads

Our authors are among the

154
Countries delivered to

TOP 1%
most cited scientists

12.2%
Contributors from top 500 universities

CLARIVATE ANALYTICS BOOK CITATION INDEX INDEXED

WEB OF SCIENCE™

Selection of our books indexed in the Book Citation Index in Web of Science™ Core Collection (BKCI)

Interested in publishing with us?
Contact book.department@intechopen.com

Numbers displayed above are based on latest data collected.
For more information visit www.intechopen.com

1

Semi-Intact Cell Systems – Application to the Analysis of Membrane Trafficking Between the Endoplasmic Reticulum and the Golgi Apparatus and of Cell Cycle-Dependent Changes in the Morphology of These Organelles

Masayuki Murata and Fumi Kano
The University of Tokyo
Japan

1. Introduction

The endoplasmic reticulum (ER) and the Golgi apparatus both maintain their specific morphology, composition, and function in spite of the exchange of proteins and lipids between the two organelles through membrane trafficking. The morphology of the Golgi apparatus is closely linked to the balance between anterograde (ER-to-Golgi) and retrograde (Golgi-to-ER) transport. It has been reported that the inhibition of anterograde transport leads to the redistribution of Golgi components to the cytoplasm or the ER (Storrie et al., 1998; Ward et al., 2001; Miles et al., 2001). Inhibition of anterograde transport at the onset of mitosis also results in the relocation of Golgi enzymes to the ER (Zaal et al., 1999; Altran-Bonnet et al., 2006), although it is controversial as to whether the Golgi becomes integrated with the ER or whether they remain separate throughout mitosis (Lowe and Barr, 2007). Thus, in living cells, the rates of anterograde and retrograde transport between the two organelles appear to have a substantial effect on the morphology of the Golgi. The effect of the balance between anterograde and retrograde transport on the morphology of the ER remains to be explored. Recently, increasing evidence has suggested that alteration in Golgi morphology during mitosis is not a passive process but rather an active one, which is highly coordinated with entry into mitosis and its progression. On the basis of the concept that cell cycle-dependent membrane trafficking between the ER and Golgi during mitosis should be tightly coupled with the changes in their morphology, it will be important to elucidate the cell cycle-dependent regulation of membrane trafficking to understand the morphological changes in more detail.

However, in general, investigation of morphological changes in the Golgi and ER during mitosis is hampered by the fact that it is difficult to observe the precise morphology of organelles in mammalian cells during mitosis by light microscopy due to the round shape of the cells. The perturbation of the distinct characteristics of the two organelles during mitosis makes it difficult to analyze the efficiency of membrane trafficking between the organelles using quantitative microscopic methods, such as fluorescence recovery after photobleaching

(FRAP), etc. In addition, the fact that concerted morphological changes occur in the organelles simultaneously and transiently in a single cell during mitosis makes it extremely difficult to dissect these changes morphologically and biochemically. The analysis is complicated further by the asynchronous progression of the cell cycle in individual cells.

Herein, we describe a novel method that addresses the above-mentioned problems, namely, a semi-intact cell assay coupled with green fluorescence protein (GFP)-visualization techniques. By using the semi-intact cell system, we can observe the morphological changes that occur in "preexisting" organelles during mitosis more easily, and, at the same time, can investigate the effects of exogenously added antibodies, drugs, and recombinant proteins on the process. By reconstituting cell cycle-dependent morphological changes in organelles using interphase or mitotic phase cytosol, we can dissect processes that occur in an orchestrated manner in the cells, morphologically and biochemically, into elementary reactions, and investigate the biochemical requirements for each reaction.

2. Semi-intact cell assays

Semi-intact cells are cells whose plasma membrane has been permeabilized with detergent or toxins, and can be referred to as "cell-type test tubes" (Fig. 1). We use a bacterial pore-forming toxin, streptolysin O (SLO), to permeabilize the cells. At 4℃, SLO binds to cholesterol in plasma membranes. At warmer temperatures, SLO assembles to form amphiphilic oligomers, which results in the generation of small, stable transmembrane pores (Bhakdi et al., 1985). SLO-induced pores are approximately 30 nm in diameter, which is sufficiently large to allow immunoglobulin to enter into the cells (immunoglobulin G: 150 kDa). Protein complexes that are larger than immunoglobulin, such as homo- or hetero-oligomers, can enter the cells through the pores as individual subunits, and the complexes are reconstituted inside the semi-intact cells. After permeabilization, almost ~80% of the cytosol flows out through the pores into the medium. However, despite this loss of cytosol, the relative intracellular configuration of the cytoskeleton and organelles or between independent organelles can be maintained because damage to the membranes of the intracellular organelles caused by entry of SLO into the semi-intact cells can be minimized by washing away any excess SLO at 4℃ before pore formation is initiated. In contrast, it is

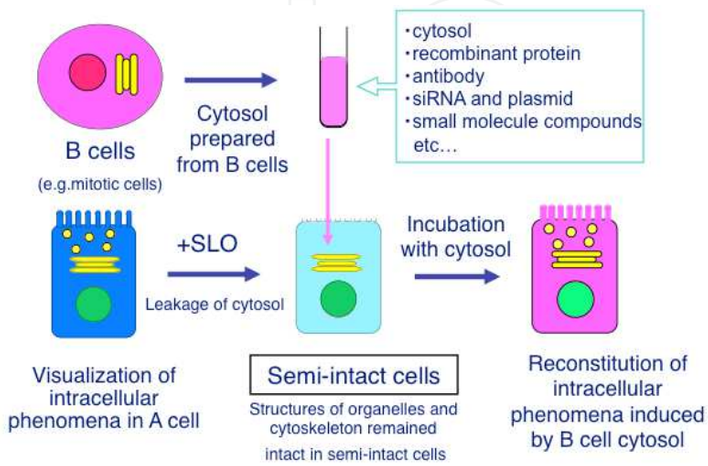

Fig. 1. A scheme of semi-intact cell assay

difficult to avoid damage to intracellular structures when cells are permeabilized with digitonin, a well-known pore-forming toxin, because digitonin-induced permeabilization is insensitive to temperature.

By exchanging cytoplasmic proteins with exogenously added proteins, antibodies or cytosol that has been prepared from cells at distinct stages of the cell cycle or differentiation, or from disease states, we can modulate the intracellular environment and reconstitute various physiological phenomena in semi-intact cells. The semi-intact cell method was originally established by Dr. Simons' group to study polarized vesicular trafficking in Madin-Darby canine kidney (MDCK) cells (Ikonen et al., 1995). We have refined the method by coupling it with GFP-visualization techniques and have established many types of assay for cell cycle-dependent changes in organelle morphology and membrane trafficking. Using our analytical system, we can manipulate intracellular conditions and then observe the resulting morphological changes in GFP-tagged organelles by fluorescence microscopy. In addition, we are able to dissect complex reaction processes in cells on a morphological basis and to investigate the biochemical requirements and kinetics of each process, for example the vesicular transport between the ER and the Golgi during mitosis. In particular, the maintenance of the integrity of the organelles and their configuration in the semi-intact cells enables us to analyze membrane trafficking in as intrinsic environment as possible.

3. Reconstitution of Golgi disassembly by mitotic cytosol in semi-intact cells

Disassembly of the Golgi during mitosis is a dynamic and highly regulated process, and is required for an equal partitioning of Golgi membranes into the two daughter cells. To investigate the biochemical requirements and kinetics of Golgi disassembly during mitosis, we reconstituted the process by adding mitotic cytosol prepared from *Xenopus* eggs to semi-intact cells and visualized it with GFP-tagged proteins (Kano et al., 2000). To this end, first, we produced the stable transfectant MDCK-GT, which continuously expresses mouse galactosyltransferase (GT) fused with GFP (GT-GFP). GT-GFP has been used to study Golgi membrane dynamics in living cells and has been characterized in detail (Cole et al., 1996). Next, we prepared semi-intact MDCK cells, which had been grown on polycarbonate membranes, incubated them with various types of cytosol, and observed the resulting changes in Golgi morphology. In semi-intact cells incubated with *Xenopus* interphase extracts, the Golgi apparatus forms perinuclear, tubular structures, which are typical of the Golgi apparatus in MDCK-GT cells. By contrast, incubation with *Xenopus* egg (M phase) extracts causes the Golgi to disassemble and the fluorescence of GT-GFP diffuses completely throughout the cytoplasm (see Fig. 2A, stage III). The diffuse staining pattern of GT-GFP that is observed, and which corresponds to small heterogeneous vesicular structures, is typical of Golgi membranes in living mitotic MDCK-GT cells.

Fluorescence microscopic observation of Golgi disassembly induced by mitotic cytosol in single MDCK-GT cells revealed that the disassembly process can be divided into three stages: stage I (intact), II (punctate), and III (dispersed) (Fig. 2). During stage I (intact), the tubular and stacked structures of a typical intact Golgi apparatus are observed in the perinuclear region through the apical to the middle part of the cells. During stage II (punctate), punctate Golgi structures are observed on mainly the apical side of the nucleus (Fig. 2A, stage II). These punctate structures are seldom seen in the basolateral cytoplasm. During stage III (dispersed), a diffuse staining pattern is observed throughout the cytoplasm

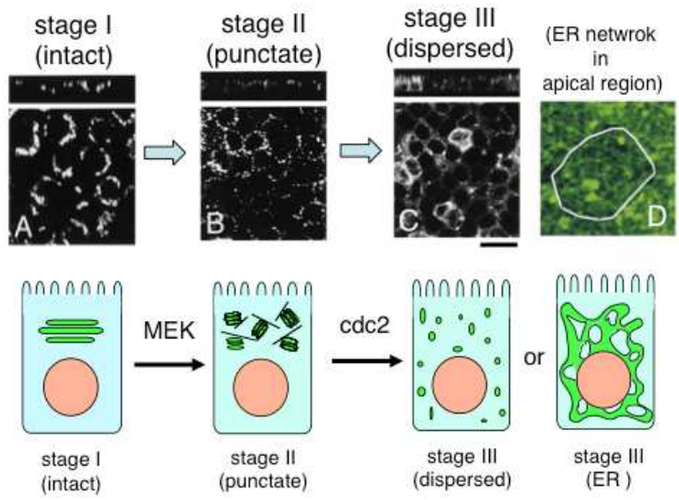

For the morphometric analysis, we divided the disassembly process into three stages based on the Golgi morphology: stage I (intact); intact perinuclear Golgi cisternae (A), stage II (punctate); punctate structures on the apical side of the nucleus (B), stage III (dispersed); highly dispersed Golgi membranes throughout the cytoplasm (C). Cells at each stage were observed by confocal microscope. The lower panel shows xy images in an apical region of the cells and the upper panel shows xz sectioning images. Bars:10 μm. In stage III cells, the relocation of Golgi component (GT-GFP) to the ER and nuclear envelopes was frequently observed in the apical region of the cells (D). Schematic model of Golgi disassembly was shown in cartoon. The morphological change in mitotic Golgi disassembly was dissected into two processes biochemically. The first process from stage I to stage II is mainly regulated by MEK1 and the second from stage II to stage III is mainly cdc2. In stage III Golgi, the vesiculated Golgi diffused throughout cytoplasm (dispersed) or the Golgi component (GT-GFP) was traslocated to the ER (ER).

Fig. 2. Morphological dissection of the Golgi disassembly process in semi-intact cells.

(Fig. 2A, stage III). Interestingly, in stage III cells, some GT-GFP appears to translocate to the ER/nuclear membranes (see the lower image in Fig. 2D). Electron microscopy confirmed the morphological differences in the Golgi apparatus between each stage. In particular, in stage II (punctate), small stacked cisternae are found in the apical region, but not in the basolateral region. The Golgi mini-stacks are 800 nm in diameter, and are associated with microtubules. Thus, the disassembly of the Golgi can be dissected into two processes morphologically (Fig. 2): the first process is the transition from stage I to stage II and the second is the transition from stage II to stage III.

Previously, two reports revealed that protein kinases, cdc2 and MEK1, are required for the Golgi disassembly process (Acharya et al., 1998; Lowe et al., 1998). However, the results of the two studies were not consistent with each other. We tested the effect of these two kinases on Golgi disassembly in semi-intact cells using mitotic cytosol that contained kinase inhibitors. Inactivation of cdc2 kinase in mitotic cytosol by the addition of butyrolactone (BL) arrests Golgi disassembly at stage II (punctate). In contrast, inactivation of MEK by PD98059 (PD) inhibits the initiation of Golgi disassembly (Fig. 3A). Next, we performed immunodepletion experiments using either cdc2- or MEK-depleted *Xenopus* egg mitotic extracts. Cdc2 was depleted from the extract by using Suc1-Sepharose beads, whereas MEK was depleted with rabbit anti-MEK polyclonal antibodies. In the presence of cdc2-depleted extract, punctate Golgi structures (stage II) are found in 90% of the cells. Furthermore, MEK-

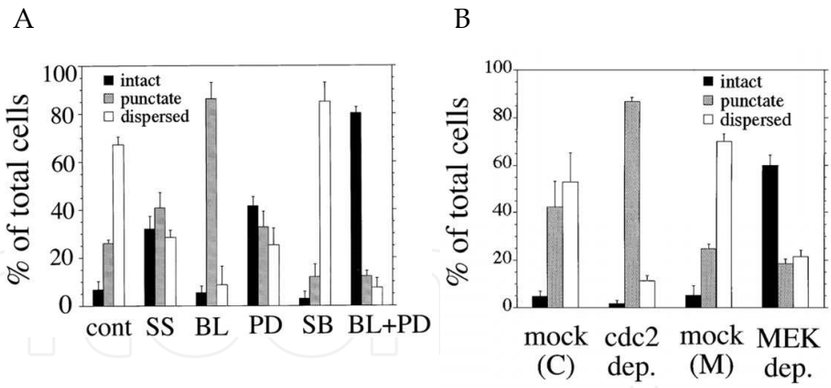

(A)Effect of protein kinase inhibitors on the Golgi disassembly. Semi-intact MDCK-GT cells were incubated with *Xenopus* egg extracts (mitotic cytosol) and ATP containing either no inhibitor (control), staurosporine (SS), butyrolactone l (BL), PD98059 (PD), SB203580 (SB), or BL+PD, respectively, at 33℃ for 80 min. After incubation, the cells were fixed and morphometric analysis was performed. The protein concentration of the extract used was 5.0 mg/ml. 300 cells were counted in three randomly selected fields, and standard deviations are shown as vertical bars. (B) Inhibition of the Golgi disassembly by cdc2- or MEK-depleted *Xenopus* egg extracts (mitotic cytsol). Mock, cdc2- or MEK-depleted *Xenopus* egg extracts were applied to semi-intact cells and incubated at 33℃ for 80 min. The cells were fixed and morphometric analysis was performed. Cdc2-depleted extracts arrested the disassembly process at stage II (punctate), and MEK-depleted extracts did so at stage I (intact).

Fig. 3. Sequential effect of MEK and cdc2 kinase on the mitotic Gogi disassembly.

depleted extract arrests the Golgi disassembly process at stage I (intact) in 60% of cells (Fig. 3B). We also confirmed the effect of each kinase on Golgi disassembly by using cdc2- or MEK-activated interphase *Xenopus* extract in semi-intact cells. The results were consistent with the effects of the kinase inhibitors and supported our model that cdc2 is responsible for the process from stage II to III, and MEK from stage I to II (Fig. 2).

However, more detailed studies using semi-intact cells revealed that each kinase does not correspond independently to the different steps. The two kinases might have overlapping functions, the first step is regulated mainly by MEK and the second step by cdc2. Interestingly, a delay in mitotic entry was observed upon inhibition of MEK1 activity. One of peripheral membrane proteins of the Golgi, GRASP55, was reported to be a substrate of MEK1 and can connect the Golgi stacks laterally into a ribbon as well as regulating mitotic progression (Feinstein and Linstedt, 2007, 2008). ERK1c and polo-like kinase-3, which are downstream of MEK1, have also been reported to contribute to Golgi disassembly during mitosis (Shaul and Seger, 2006; Xie et al., 2004). On the other hand, another peripheral Golgi protein GRASP65, which is known to function in cisternal stacking as well as in the lateral linking of stacks, was reported to be phosphorylated by cdc2 and the phosphorylation was required for entry into mitosis (Yoshimura et al., 2005; Preisinger, et al., 2005). Collectively, these results confirm our findings that the Golgi mini-stacks in stage II are generated from intact Golgi by the activation of MEK1, and the dispersed Golgi observed in stage III from the Golgi mini-stacks by the activation of cdc2. In addition, MEK1- or cdc2-dependent changes in Golgi morphology might be essential for mitotic entry.

Cdc2 is also likely to be involved in COPI-dependent disassembly of the Golgi during mitosis. At the onset of mitosis, the peripheral Golgi protein GM130 is known to be

phosphorylated by cdc2; GM130 phosphorylation inhibits p115-dependent tethering and the subsequent fusion of Golgi-derived COPI-dependent vesicles to the Golgi cisternae (Lowe et al., 2000). Continuous budding without the fusion of new vesicles might reduce the cisternae rapidly and facilitate the mitotic disassembly of the Golgi. Thus, it is likely that the roles of MEK1 and cdc2 in mitotic Golgi disassembly involve both COPI-dependent and -independent processes.

4. Reconstitution of cell cycle-dependent morphological changes in the ER network in semi-intact cells

To investigate the cell cycle-dependent changes in the morphology of the ER network in mammalian cells, we created a clonal cell line derived from Chinese Hamster Ovary (CHO) cells that constitutively express GFP-HSP47 (CHO-HSP) and have a flat morphology when grown in culture, such that the cytoplasm is easy to visualize (Fig. 4). Using confocal microscopy, we found that, during interphase, GFP-HSP47 in CHO-HSP cells is associated with polygonal structures with three-way junctions that are located at the periphery of the cells and in the cisternae in the perinuclear region (Fig. 4, interphase). Interestingly, at the onset of mitosis, the ER appears to retain its network structure rather than being disrupted into vesicles, in contrast to the Golgi apparatus (Fig. 4, mitotic phase). Further observation with the fluorescence microscope revealed that the ER is partially severed at the onset of mitosis. In fact, recent advances in quantitative confocal and electron microscopy (EM) analyses by the application of electron tomography techniques have revealed that, in the mitotic ER, the tubules are shorter and more branched and cisternae are extended in comparison with the ER during interphase (Puhka et al., 2007; Lu et al., 2009). These results confirm our observations by fluorescence microscopy, and show that the cell cycle-dependent changes in ER morphology seem to be completely different from those in Golgi morphology.

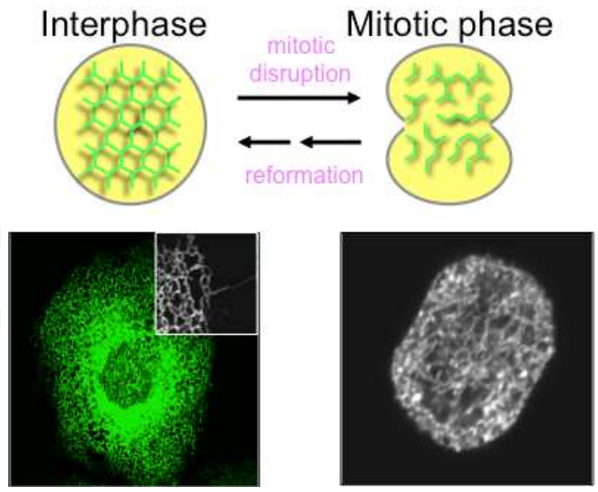

The ER network connected with three-way junctions is visible in interphase CHO-HSP cells (see inset of image for interphase ER network). The ER tubules fuse with each other to make new three-way junctions. At the onset of mitosis, the ER network appears to retain the network structure, and dose not seem to be disrupted into vesicles like mitotic Golgi vesicules. Further observation by fluorescence microscope enables us to discover the ER is partially severed during mitosis.

Fig. 4. Cell cycle-dependent morphological changes in the ER network.

We reconstituted the cell cycle-dependent changes in ER morphology in semi-intact cells, identified regulatory factors, and elucidated the mechanisms that underlie the morphological changes (Kano et al., 2005a and b). First, we preincubated CHO-HSP cells with nocodazole to disrupt the microtubules and then permeabilized them with SLO. Then, we incubated the semi-intact CHO-HSP cells with mitotic cytosol, which was prepared from synchronized mitotic L5178Y cells, and found that the continuous network of the ER was partially severed, as was seen in intact mitotic CHO-HSP cells. As shown in Fig. 5A, in the presence of mitotic cytosol, the ER network is partially disrupted and, thus, the connections between ER tubules are broken. In contrast, in the presence of interphase cytosol, the ER network remains intact. To quantify the partial disruption of the ER, we counted the number of three-way junctions per defined area (Fig. 5B). Mitotic cytosol induces a decrease in the number of three-way junctions, which signifies that the ER network is disrupted. In addition, we found that when nocodazole is not added the ER network remains intact even in the presence of mitotic cytosol. These results suggest that microtubules strengthen the integrity of the ER network, and that both depolymerization of microtubules and exposure to mitotic cytosol are necessary for the complete disruption of the ER network. Interestingly, we frequently observed dynamic tubulation/bifurcation of ER tubules in the presence of either mitotic or interphase cytosol, which suggests that partial disruption of the ER network by mitotic cytosol results from inhibition of the fusion process, rather than inhibition of tubulation/bifurcation (unpublished data).

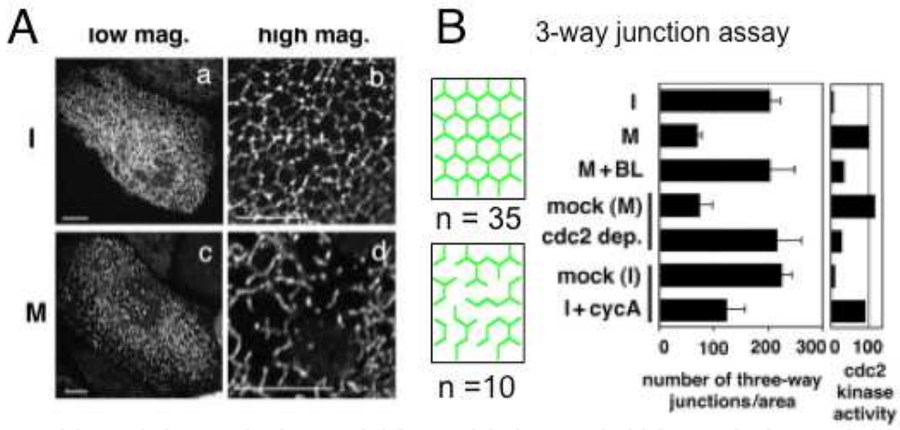

(A) CHO-HSP cells were pretreated with nocodazole and permeabilized with SLO. The cells were incubated with interphase (a, b) or mitotic (c, d) cytosol at 32℃ for 40 min, and observed under a confocal microscope at low(a, c) or high (b, d) magnification. Bar = 10 μm (low mag.), 5 μm (high mag.). (B) After the incubation, to quantify the partial disruption of the ER network, we counted the number of three-way junctions per area and compared (three-way junction assay). Nocodazole-treated semi-intact CHO-HSP cells were incubated with interphase cytosol (I, cdc2 kinase activity was 0.27 units/μL), mitotic cytosol (M, 5.68 units/μL), mitotic cytosol containing 30 μm butyrolactone1 (M+BL, 1.86 units/μL), mock mitotic cytosol (mock (M), 6.55 units/μL), cdc2-depleted mitotic cytosol (cdc2 dep.1.66 units/μL), mock interphase cytosol (mock (I), 0.52 units/μL), or interphase cytosol treated with cyclin A (I+cycA, 5.18 units/μL). After the incubation, three-way junction assay was performed. Cdc2 kinase activity in each reaction mixture (means from two independent measurements) is shown in the right hand column, where 100% represents the value of cdc2 kinase activity in mitotic cytosol. Cdc2 kinase activity correlated with the disruption of ER network.

Fig. 5. Disruption of the ER network by mitotic cytosol in semi-intact CHO-HSP cells.

With regard to the fusion process, some cytosolic proteins or their regulators that are downstream of cdc2 kinase are thought to be inactive in mitotic cytosol (Lowe et al. 1998; Kano et al. 2000a). Extrapolating from these findings, the disruption of the ER network by mitotic cytosol *in vitro* could also result from the blocking of fusion events by cdc2 kinase-mediated phosphorylation. One of the candidates for this inhibition is p47, a cofactor of p97, which mediates the fusion of Golgi membranes (Kondo et al. 1997). More recently, Uchiyama et al. (2003) found that Ser140 of p47 was selectively phosphorylated by cdc2 kinase and that this phosphorylation was involved in Golgi disassembly during mitosis. They also found that a non-phosphorylated form of p47, p47 (S140A), which is referred to as p47NP, inhibited mitotic Golgi disassembly. Phosphorylation of p47 by cdc2 dissociated the p97/p47 fusion complex from membranes, which has the potential to inhibit membrane fusion between ER tubules. To test this, we investigated the effect of p47NP on the partial disruption of the ER network that is induced by mitotic cytosol in semi-intact cells. In the presence of p97/p47NP, the partial disruption of the ER network was inhibited. Therefore, we concluded that the disruption of the ER during mitosis depends on phosphorylation of p47 by cdc2 (Fig. 6).

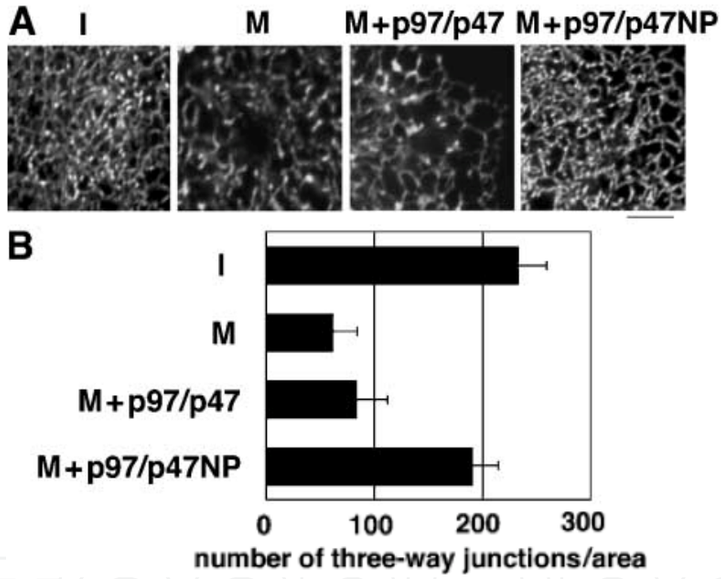

(A) Nocodazole-treated semi-intact CHO-HSP cells were incubated with interphase cytosol (I), mitotic cytosol (M), mitotic cytosol +recombinant p97 and p47 (M+p97/p47), mitotic cytosol +p97 and mutated p47S140 A (M+p97/p47NP), at 32℃ for 40 min. The cells were observed by confocal microscopy (A) and were subjected to a three-way junction assay (B). Bar = 10 μm.

Fig. 6. Phosphorylation of p47 by cdc2 results in the disruption of the ER network.

Next, we reconstituted the reformation of the ER network after cell division (Kano et al., 2005b). First, semi-intact CHO-HSP cells were incubated with mitotic cytosol to induce the partial disruption of the ER network. After the mitotic cytosol had been removed, the semi-intact cells were incubated with interphase cytosol, which led to the reformation of the ER network (Fig. 7). This reformation is induced by the fusion protein complexes in the interphase cytosol. There are two well-characterized protein complexes involved in intracellular membrane fusion: the NSF/SNAP complex and the p97/p47 complex.

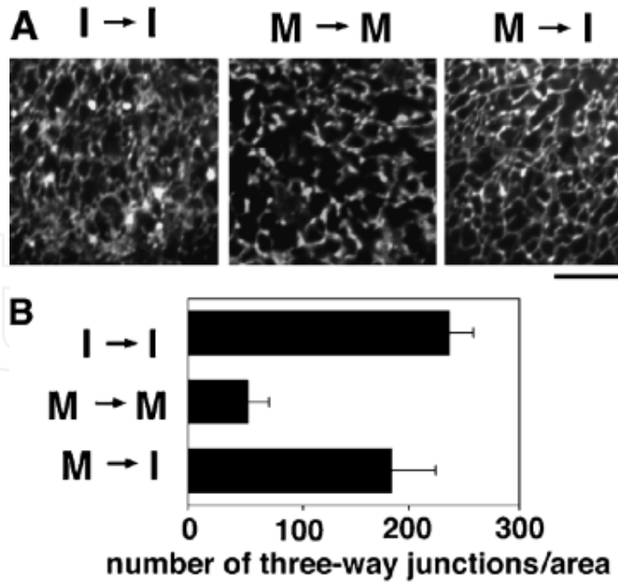

Nocodazole-treated, semi-intact CHO-HSP cells were incubated with interphase (I→) or mitotic (M→) cytosol at 32℃ for 40 min. After washing out the cytosol with cold TB, the cells were further incubated with interphase (I→I, M→I), or mitotic cytosol (M→M). The cells were fixed, and images were acquired by confocal microscopy (A) or were subjected to a three-way junction assay (B). Bar = 10 μm.

Fig. 7. Reformation of the ER network from the disrupted ER tubules by interphase cytosol.

Antibodies against NSF or p47 that inhibit NSF/SNAP- or p97/p47-mediated intracellular membrane fusion also inhibit the reformation of the ER that is induced by interphase cytosol, which indicates that the reformation process is regulated by both the NSF/SNAP complex and the p97/p47 complex (Fig. 8A). These results were confirmed by the following experiment. Both NSF and p97 are sensitive to the alkylating reagent N-ethylmaleimide (NEM), and NEM treatment inactivates the fusion of Golgi vesicles. Interphase cytosol was treated with NEM and the effect of the cytosol on ER reformation was examined. As expected, the NEM-treated cytosol did not induce reformation of the ER network. However, the addition of recombinant NSF/SNAP and p97/p47 complexes to the NEM-treated interphase cytosol restored its ability to induce reformation of the network (Fig. 8B). Next, we incubated semi-intact CHO-HSP cells in which the ER network had been disrupted by the addition of mitotic cytosol with a mixture of NSF/SNAP and p97/p47 complexes only (without NEM-treated cytosol), and found that the ER network was not reformed fully. This suggested that other factor(s) in NEM-treated cytosol are required for the ER reformation. We found that VCIP135, a deubiquitinating enzyme that transiently associates with the p97/p47 complex, is necessary for the reformation but p115, which plays a role in tethering Golgi-derived vesicles to Golgi cisternae, is not. Consequently, this result signified that the NSF/SNAP and p97/p47/VCIP135 complexes are the minimal factors required for the ER reformation. In addition, we found that the order of action of the NSF/SNAP and p97/p47/VCIP135 complexes is crucial for the reformation (Fig. 8B). When we incubated the disrupted ER network with the NSF/SNAP complex first, and then the p97/p47/VCIP135 complex, the ER network reformed. However, when the disrupted network was incubated with the p97/p47/VCIP135 complex first, and then the NSF/SNAP complex, the network remained disrupted.

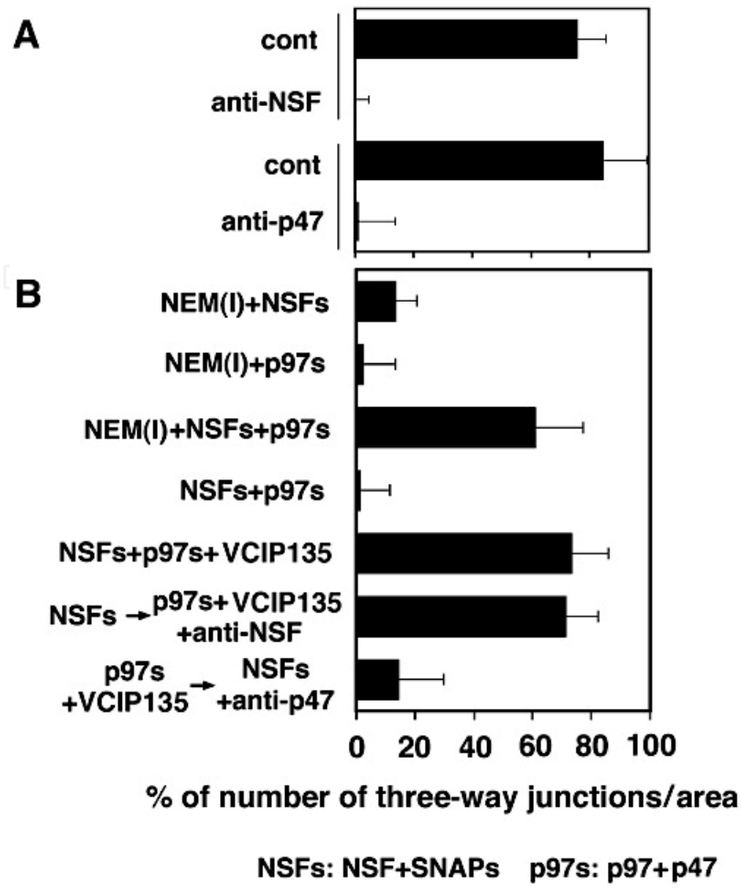

(A) The ER reformation assay was performed using interphase cytosol with pre-immune serum (cont), interphase cytosol with anti-NSF antibody (anti-NSF), interphase cytosol with anti-p47 antibody (anti-p47). (B) The ER reformation assay was performed using NEM-treated interphase cytosol (NEM(I)), NEM-treated interphase cytosol with NSF+SNAPs (NEM(I)+NSFs), NEM(I) cytosol with p97+p47 (NEM(I) +p97s), NEM(I) cytosol with both (NEM(I)+NSFs+p97s), NSFs+p97s, or NSFs+ p97s+VCIP135 at 32℃ for 80 min. When cells were incubated in a sequential manner, semi-intact cells, treated with mitotic cytosol were incubated with NSFs or p97s+VCIP135 at 32℃ for 40 min, washed with 2M KCl in TB for 25 min, then further incubated with p97s+VCIP135+anti-NSF antibodies or NSFs+anti-p47 antibodies at 32℃ for 40 min, respectively (NSFs→p97s+VCIP135+anti-NSF, p97s+VCIP135→NSFs+anti-p47). The efficiency of ER network reformation under each condition were estimated by three-way junction assay.

Fig. 8. NSF/SNAP complex and p97/p47 complex are required for ER network reformation.

Fig. 9 shows a schematic model of the cell cycle-dependent morphological changes in the ER network. As mentioned above, we found that the cdc2-dependent phosphorylation of p47 induces the partial disruption of the ER network during mitosis. Interestingly, the reformation of the ER network is not accomplished by a single fusion reaction, but rather requires two sequential fusion reactions. The first fusion event is mediated by the NSF/SNAP complex, which creates intermediate membranous structures between the disrupted ER tubules. These intermediate structures can be observed only by EM. The second fusion event is mediated by the p97/p47/VCIP135 complex, which induces the fusion of connected ER tubules to form three-way junctions.

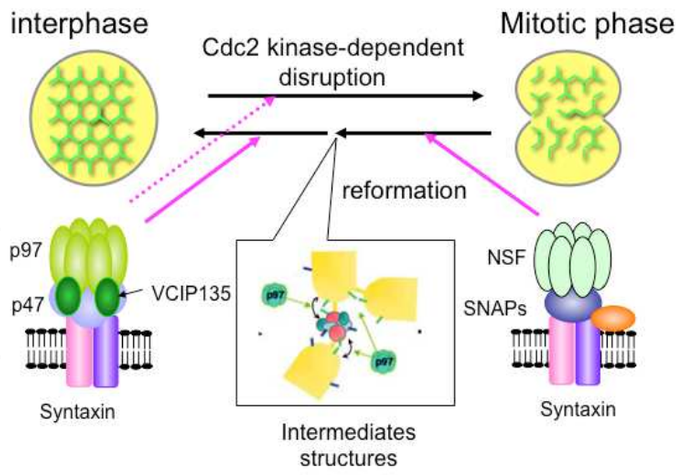

The process of ER network reformation was dissected into two elementary process. Firstly, disrupted ER tubules, induced by mitotic cytosol, are connected by two types of intermediate structures; fine junctions or vesicle aggregates. Both of these intermediate structures are created by NSFcomplex and may function as a "connecting" system. Secondly, the "connected" ER tubules completely fuse with each other directly or through the intermediate structures indirectly to form three-way junctions. This process is dependent on p97/p47 and VCIP135. Syntaxin family is involved in both NSF- and p97-mediated fusion processes with unidentified vesicle-localizing receptors.

Fig. 9. Schematic model for the ER network reformation process.

Given that the NSF/SNAP and p97/p47/VCIP135 complexes are required for the reassembly of the Golgi apparatus after mitosis, it is not surprising that both fusion complexes play a crucial role in the reformation of disrupted ER networks. During Golgi reassembly, the p97/p47 complex is reported to generate single, long cisternae, whereas the NSF/SNAP complex fuses membranes into much shorter but stacked cisternae (Tang et al., 2008). As described above, in our EM study of ER reformation, fine junctions that connected two individual tubules or vesicle aggregates were frequently observed as intermediate structures between the disrupted ER tubules. It is likely that these intermediate structures are produced by the NSF/SNAP complex from Golgi vesicles. The intermediates disappeared within 5 min of incubation with the p97/p47/VCIP135 complex, and formed long tubular structures with bifurcations (three-way junctions), which were also seen in intact cells. Thus, the two fusion complexes seem to generate similar membrane products during both Golgi reassembly and ER reformation.

It might be important to note that p47 contains a UBA (ubiquitin-associated) domain and recruits p97 to monoubiquitinated substrates (Meyer et al., 2002). Taking into consideration the fact that VCIP135 is a deubiquitinating enzyme, regulation of the balance between ubiquitination-deubiquitination might be involved in the disassembly and reformation of the ER network during mitosis, as is the case for Golgi reassembly.

5. Reconstitution of cell cycle-dependent anterograde or retrograde transport between the ER and the Golgi in semi-intact cells

Using our semi-intact cell system, we reconstituted cell cycle-dependent vesicular transport between the ER and the Golgi (Kano et al., 2009). To measure the vesicular transport

between the ER and Golgi, we used FRAP. Firstly, we established CHO-GT cells, in which GT-GFP was stably expressed. GT-GFP is trafficked between the ER and Golgi by vesicular transport, but in the steady state, GT-GFP is mainly localized to the Golgi apparatus, with a small proportion in the ER. For FRAP, the fluorescence of GT-GFP in the Golgi region is bleached by repetitive laser illumination. After bleaching, fluorescence in the Golgi area is recovered due to anterograde transport of GT-GFP from the ER to the Golgi. By measuring the fluorescence recovery in the Golgi area, we can estimate the extent of transport of GT-GFP from the ER to the Golgi (Fig.10). To examine retrograde transport from the Golgi to the ER, the fluorescence in the ER region is bleached and the fluorescence recovery of the ER (whole area of the cell except for the nucleus) is determined (Fig. 11). We confirmed that fluorescence recovery in the ER region is not due to the appearance of newly synthesized GT-GFP by pretreating the cells with cycloheximide to inhibit protein synthesis. In fact, when both the Golgi and ER regions were photobleached simultaneously, no fluorescence recovery was observed in the ER region (F. K., unpublished results). Figure 12 shows representative kinetic curves for the anterograde and retrograde transport of GT-GFP that were obtained from the assay. In the presence of mitotic cytosol, anterograde transport is

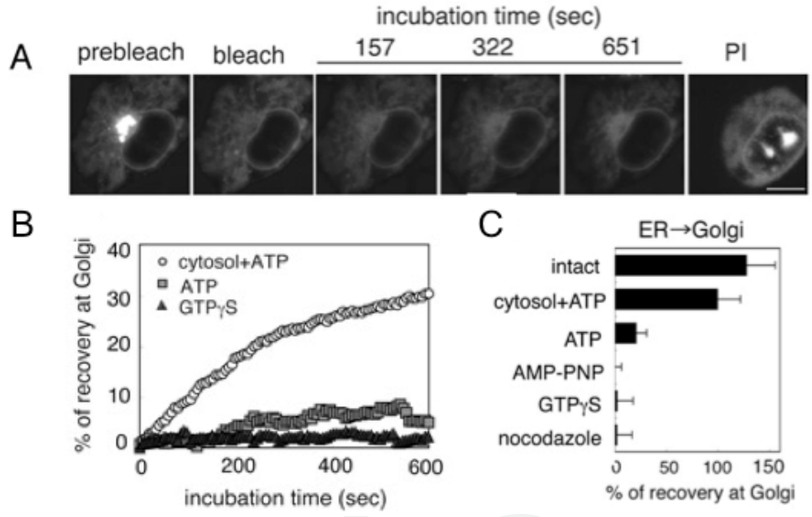

(A) CHO-GT cells were pretreated with cycloheximide (CHX). GT-GFP in the Golgi region of a single semi-intact CHO-GT cell was photobleached by laser illumination (bleach). The cell was incubated in the presence of cytosol/ATP for the indicated times (sec). PI, propidium iodide. Scale bar: 10 μm. (B) Kinetics of fluorescence recovery after photobleaching in the Golgi region in the presence of cytosol/ATP (cytosol+ATP), an ATP regenerating system only (ATP), or cytosol/ATP plus 1 mM GTPγS (GTPγS). After CHX treatment, GT-GFP in the Golgi region was photobleached, and the semi-intact cells were incubated at 32°C for 10 minutes in the presence of cytosol/ATP. Cells were then treated with 10 μg/ml brefeldin A (BFA) for 30 minutes to relocate the Golgi-localized GT-GFP to the ER. This indicated that the recovered fluorescent structure was the Golgi apparatus. (C) Semi-intact CHO-GT cells that had been treated with CHX were incubated with cytosol/ATP (cytosol+ATP), an ATP regenerating system only (ATP), cytosol plus 1 mM AMP-PNP (AMP-PNP), or cytosol/ATP plus 1 mM GTPγS (GTPγS), and then subjected to the anterograde transport assay. In addition, intact CHO-GT cells were treated with nocodazole (nocodazole), and then subjected to the anterograde transport assay. In our anterograde transport assay, we confirmed that the fluorescence recovery in the Golgi was attributable to the anterograde transport of GT-GFP alone, and was not affected by retrograde transport from the Golgi.

Fig. 10. Reconstitution of anterograde transport of GT-GFP in semi-intact cells.

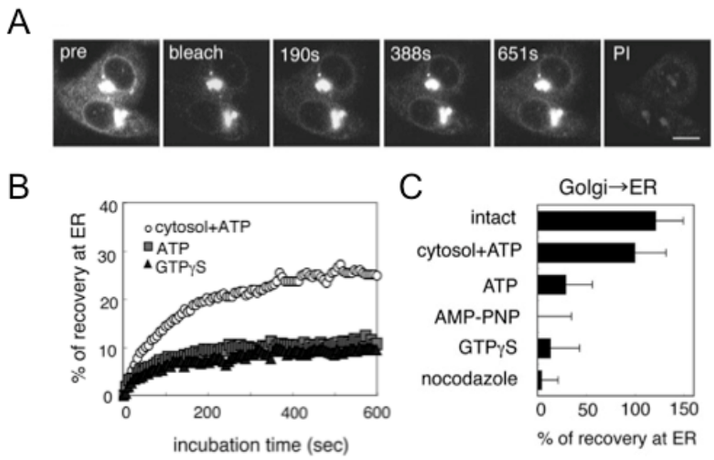

(A) After cycloheximide (CHX) treatment to inhibit protein synthesis, GT-GFP within the ER region was photobleached by laser illumination (bleach). Semi-intact cells were then incubated with cytosol/ATP at 32°C for the indicated times (sec). PI represents propidium iodide. Scale bar: 10 μm. (B) Semi-intact CHO-GT cells that had been treated with CHX were incubated with cytosol/ATP (cytosol+ATP), an ATP regenerating system only (ATP), cytosol plus 1 mM AMP-PNP (AMP-PNP), or cytosol/ATP plus 1 mM GTPγS (GTPγS), and then subjected to the retrograde transport assay. In addition, intact CHO-GT cells were treated with nocodazole (nocodazole), and then subjected to the retrograde transport assay.

Fig. 11. Reconstitution of the retrograde transport of GT-GFP in semi-intact cells.

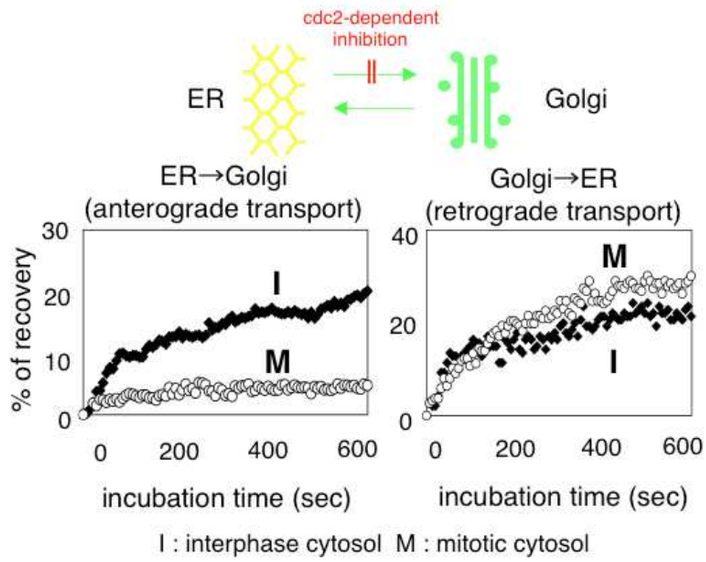

The antrograde or retrograde transport assay described in Fig.10 and 11 were performed using interphase or mitotic cytosol. In the transport kinetics graph, representative kinetics of fluorescence recovery after photobleaching was shown in the presence of interphase (I) or mitotic (M) cytosol and ATP-generating system. In the presence of mitotic cytosol, the anterograde transport was selectively inhibited, but the retrograde one remained intact. By using cdc2-depleted mitotic cytosol, we also found that the mitotic inhibition of the anterograde transport was dependent on cdc2 kinase.

Fig. 12. Reconstitution of anterograde or retrograde transport of GT-GFP in the presence of interphase or mitotic cytosol.

selectively inhibited, whereas retrograde transport remains intact. In addition, we found that cdc2-depleted mitotic cytosol induces anterograde transport normally, which indicates that the mitotic inhibition of anterograde transport is also dependent on cdc2 kinase.

Next, we examined which process in the anterograde transport is inhibited by mitotic cytosol. For this purpose, we focused on the cell cycle-dependent changes in the morphology of ER exit sites. ER exit sites (ERES) are specialized membrane domains in the ER from which vesicles that contain cargo proteins destined for the Golgi bud. To visualize ERES, we established CHO-YIP cells, which stably express the ERES resident protein Yip1A as a fusion with GFP (Fig. 13A). Yip1A belongs to the Yip family of proteins, which contain the Yip domain, and is thought to have a role in membrane trafficking. Although we have confirmed recently that endogenous Yip1A is localized to the ERGIC (ER-Golgi intermediate compartment) by immunofluorescence using an anti-Yip1A antibody, we also observed that in CHO cells Yip1A fused with GFP accumulates at ERES as bright punctate structures throughout the ER network (Fig. 13A). By observing the morphological changes in ERES that occur in CHO-YIP cells during the cell cycle, we found that ERES are disrupted and Yip1A-GFP is dispersed throughout the ER network at the onset of mitosis. After cell division, the diffuse Yip1A-GFP fluorescence accumulates at the ERES in daughter cells (Fig. 13B). The disruption of ERES during mitosis suggests that vesicle budding from ERES does not occur during mitosis. To test this, we reconstituted the mitotic disassembly of ERES by adding mitotic cytosol to semi-intact CHO-YIP cells and investigated the biochemical requirements for the disassembly process. As shown in Fig. 14, the addition of mitotic

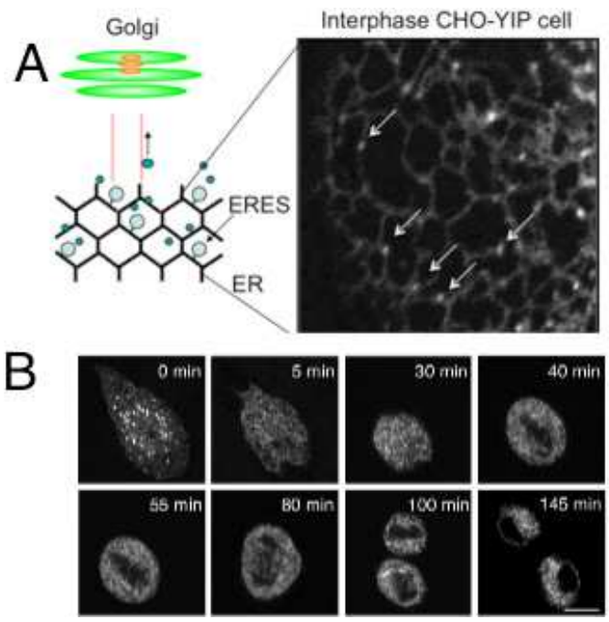

(A) ERES, which is the specialized membrane domain in the endoplasmic reticulum where vesicles that contained cargo proteins budded, were visualized using Yip1A-GFP in CHO-YIP cells (arrows). In CHO-YIP cells the majority of the Yip1A-GFP fluorescence accumulated as bright punctate structures throughout the ER network. (B) Observing the morphological changes of the ERES during cell cycle. The ERES was disrupted and Yip1A-GFP was dispersed throughout the ER network at the onset of mitosis. This proves that the vesicle budding at ERES failed to occur during mitosis.

Fig. 13. ER exit sites (ERES) visualized by Yip1A-GFP in CHO-YIP cells.

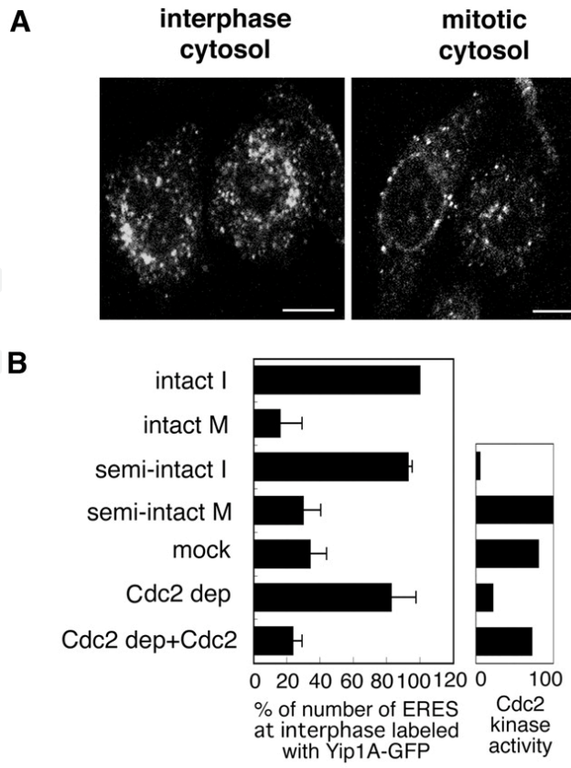

(A) Semi-intact CHO-YIP cells were incubated with interphase or mitotic cytosol with an ATP-regenerating system at 32°C for 20 min and then viewed by a confocal microscope. Bar, 10μm. (B) Number of ERES in interphase cells (intact I) or mitotic cells (intact M) was calculated using the ERES disassembly assay (see in details in Kano et al., 2004). Semi-intact CHO-YIP cells were incubated with interphase cytosol (semi-intact I), mitotic cytosol (semi-intact M), mock mitotic cytosol (mock), Cdc2-depleted mitotic cytosol (Cdc2 dep), or Cdc2-depleted mitotic cytosol plus 72 U of Cdc2/cyclin B (Cdc2 dep +Cdc2). After the incubation, the cells were subjected to the ERES disassembly assay. Cdc2 kinase activity in each reaction mixture (means from two independent measurements) is shown in the right hand column, in which 100% represents the value of Cdc2 kinase activity in mitotic cytosol. Three independent assays were performed and the means and standard deviations are plotted in the graph.

Fig. 14. Biochemical requirements for ERES disassembly by mitotic cytosol.

cytosol causes ERES to disassemble and reduces their number significantly, perhaps by as much as 80%, as compared with interphase cytosol. In addition, cdc2-depleted mitotic cytosol does not induce the disassembly of ERES. Furthermore, addition of recombinant cdc2 kinase to mitotic cytosol from which cdc2 has been depleted restores the ability of the cytosol to induce disassembly. Taken together, the results show that the mitotic disruption of ERES also depends on the activation of cdc2 kinase.

One of the target proteins of cdc2 kinase that might be involved in the mitotic disassembly of ERES is p47. p47 has been reported to play a crucial role in the *de novo* formation of ERES *in vitro* (Roy et al., 2000) and in the formation of ER network from microsomal membrane vesicles (Hetzer et al., 2001) or the reformation of disrupted ER networks after mitosis (Kano et al., 2005b). On the basis of these results, we hypothesized that p47 is also required for the maintenance of ERES and that the disassembly of preexisting ERES is

controlled by phosphorylation of p47, in a cdc2-dependent manner. To test this, we assayed ERES disassembly in semi-intact cells incubated with mitotic cytosol and ATP in the presence of p97 and p47 or p97 and p47NP. The mitotic disassembly of ERES is partially blocked in the presence of p97 and p47. However, in the presence of p97 and p47NP, disassembly is completely inhibited. We also examined the effect of p97/p47NP on the dissociation of Sec13, one of the components of COPII vesicles, from ERES, and confirmed that the dissociation of Sec13 induced by mitotic cytosol is substantially inhibited by p97/p47NP and partially inhibited by p97/p47. These results suggest that the cdc2-dependent phosphorylation of p47 plays a crucial role in the disassembly of preexisting ERES. We assumed that the complete inhibition of the disassembly by p97/p47NP would preserve the anterograde transport of VSVGts045-GFP. However, anterograde transport is only partially restored under these conditions. Other factors, such as microtubule-dependent motor proteins, probably contribute to the specific block of anterograde transport during mitosis.

These results suggest that the phosphorylation of p47 triggers the disassembly of ERES and corresponding inhibition of anterograde transport. Recently, Hughes and Stephens (2010) found that Sec16A, which interacts with Sec23 and Sec13 and serves to optimize COPII assembly at ERES, remains associated with ERES throughout mitosis. They suggested that the Sec16A at ERES facilitates full assembly of COPII vesicles during anaphase, which precedes the reassembly of the Golgi apparatus during telophase.

The mechanism that regulates the partitioning of Golgi vesicles during mitosis remains controversial. Two mechanisms have been proposed: 1) the Golgi fragmentation model by Warren (1993) and 2) the Golgi absorption model by Zaal et al. (1999). In the first model, the distinction between the Golgi and the ER persists during mitosis and the components of the two organelles are inherited independently. In the second model, some components of the Golgi translocate to and merge with the ER, and thus are inherited as components of the ER/nuclear envelope. Although both models are supported extensively by evidence from several elegant experimental systems, the issue remains to be resolved (Atlan-Bonnet et al., 2006; Bartz et al., 2008). Our retrograde transport assay using semi-intact cells revealed that mitotic cytosol is competent to induce mitotic processes, including vesicle budding, vesicle transport, and vesicle fusion, and results in the translocation of Golgi components to the ER. In addition, as described in the experiments on mitotic Golgi disassembly in semi-intact cells, during the late steps of Golgi disassembly (most likely at stage III), substantial amounts of GT-GFP can be observed in the nuclear envelope and ER-like networks, having translocated from the Golgi. Furthermore, staining of the nuclear envelope with GT-GFP is more extensive at stage III than at stage II. These findings suggest that the relocation of Golgi components (in this case, GT-GFP) to the ER does occur during Golgi disassembly, at least in mitotic MDCK cells, and most likely takes place during the later steps of disassembly. However, it is difficult for us to address whether the Golgi membranes are converted into vesicles during disassembly or fuse with the ER. Given that GT-GFP is known to be a cargo for COPI-independent retrograde transport from the Golgi to the ER, the translocation of GT-GFP to the ER during mitosis might be attributed to COPI-independent Golgi disassembly, which is frequently observed as the transformation of cisternae into an extensive tubular network in a cell-free system or semi-intact cells (Misteli et al., 1995).

6. Schematic model for the coupling of ER and Golgi biogenesis to vesicular transport during the cell cycle

On the basis of our results and those of others, we have developed a hypothesis about the relationship between the cell cycle-dependent morphological changes in the ER and Golgi and the regulation of vesicular transport between the ER and Golgi in mammalian cells (Fig. 15). During the earlier steps of mitosis, activation of cdc2 kinase induces the phosphorylation of p47 and other proteins. The phosphorylated p47 causes the disassembly or vesiculation of the Golgi apparatus, and concurrently causes the partial severance of the ER network and disassembly of ERES. The disassembly of ERES inhibits anterograde transport from the ER to the Golgi, but retrograde transport remains intact. As a result, some components of the Golgi apparatus translocate to the ER network during the early phase of mitosis. The severed ER network and vesiculated Golgi membranes are easily distributed into two daughter cells, on a stochastic basis. After mitosis, the vesiculated Golgi membranes fuse with one another and reform intact Golgi stacks. In addition, the severed ER tubules are quickly reformed into a continuous ER network. These processes of reformation depend on the membrane fusion reactions that are mediated by the NSF/SNAP and p97/p47/VCIP135 systems. It is very interesting that, during Golgi reformation after mitosis, the two membrane fusion complexes act concurrently, whereas, in the reformation of the ER network, the two complexes act sequentially. It is likely that the reformation of ERES might involve the dephosphorylation of p47 given that the activity of cdc2 kinase diminishes in late mitosis and anterograde transport resumes in conjunction with Golgi reassembly and ER reformation after cell division. Probably, Sec16A, which remains associated with ERES throughout mitosis, facilitates the resumption of anterograde transport.

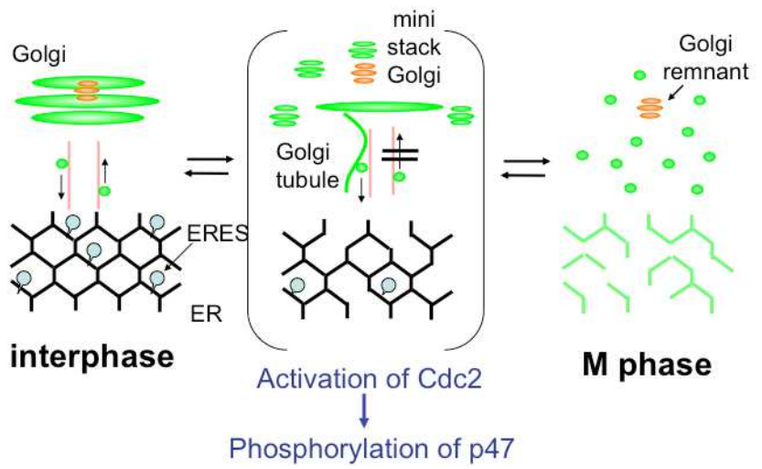

Fig. 15. Schematic model of cell cycle-dependent organelle morphology coupling and membrane traffics.

7. Complementary usage of *in vitro* reconstitution assays and semi-intact cell assay

In mitotic cells, orchestrated changes in Golgi and ER morphology occur simultaneously and are coupled with the re-arrangement of the cytoskeleton. Thus, it is likely that the roles

of certain proteins in mitotic cells might be masked. Our semi-intact cell assay is suitable for investigating the biochemical requirements of specific processes, which might be masked by the orchestrated physiological reactions. For example, the ER disassembly assay revealed that a p97/p47-mediated fusion process plays a crucial role in the maintenance of the ER network when microtubules are disrupted by nocodazole. In another case, the ER reformation assay revealed that reformation of the ER is accomplished even in nocodazole-treated semi-intact cells. When microtubules are intact, the contribution of the fusion process to the maintenance or reformation of the ER network appears to be masked. Our transport assay also revealed that, even in the presence of mitotic cytosol, the retrograde transport of GT-GFP occurs normally when microtubules remain intact, but ERES are disassembled easily under these conditions (Fig.14). The findings suggest that mitotic cytosol can facilitate retrograde transport as long as microtubule integrity is maintained, but anterograde transport ceases rapidly in the presence of mitotic cytosol. Thus, the ability to manipulate the cytoskeleton easily in semi-intact cell systems will be useful in elucidating the role of the cytoskeleton in the process of morphological change in organelles or membrane trafficking during mitosis.

Many *in vitro* reconstitution assays have been developed to investigate the biochemical requirements for the maintenance or mitotic alteration of Golgi or ER morphology, and a variety of key molecules have been identified using these methods (Acharya et al.,1998; Lowe et al., 1998,2000; Hetzer et al., 2001). Our semi-intact cell assays will be useful for confirming the precise role of these molecules in the maintenance or alteration of morphology under conditions in which the configuration between organelles and the cytoskeleton is almost the same as in living cells. Thus, our assays will provide additional spatial information about where the molecules function or where the biological reactions occur in cells. By applying the Golgi disassembly assay in semi-intact cells, we found that punctate Golgi structures (Fig. 3, stage II Golgi), which are produced mainly by MEK1 from cisternal Golgi and are referred as to Golgi mini-stacks, are found mainly on the apical side of the nucleus and are associated with apical microtubules. Given that the spatial configuration of the cell is virtually unaffected in semi-intact cells, the semi-intact cell assays are superior to *in vitro* reconstitution assays for investigating the anterograde or retrograde transport between the Golgi and the ER.

There are some differences between *in vitro* reconstitution systems and our semi-intact cell system. For example, an *in vitro* ER formation assay developed by Dreier and Rapoport (2000) revealed that the characteristic polygonal structure of the ER was formed from microsomal membranes. However, the *in vitro* network produced in their assay appeared to be slightly different from the ER network formed in CHO-HSP cells. The length of one side of the three-way junctions was approximately 5 μm in their reconstituted network, compared to 1–1.5 μm in our intact or semi-intact CHO-HSP cells. We have frequently observed that this length varies with the cellular conditions. For example, following serum starvation, the length appears to be greater than 5 μm (F. K., unpublished data).

Collectively, our semi-intact cell assays are superior to *in vitro* reconstitution assays in terms of obtaining morphological or spatial information, but *in vitro* assays are more appropriate for determining biochemical requirements than semi-intact cell assays. Using both assays together will enable us to identify the key molecules involved in morphological changes, which might be masked by the orchestrated processes that occur

during mitosis, and to elucidate the underlying mechanisms more precisely on the basis of morphological data.

8. Conclusions

The mechanisms that regulate the cell cycle-dependent changes in Golgi morphology in mammalian cells have been studied extensively (see reviews, Wei & Seemann, 2009). In terms of the relationship between Golgi morphology and membrane trafficking, the size and morphology of the Golgi are thought to be determined mainly by the membrane influx/efflux ratio. Thus, the characteristic features of Golgi morphology could depend on the stage of the cell cycle, cell type or intracellular conditions (Sengupta & Linstedt, 2011). In contrast, many aspects of the regulation of the morphology of the ER network remain poorly understood. The ratio of membrane influx/efflux at the ER seems to affect ER morphology less than the ratio at the Golgi affects Golgi morphology because a large amount of membrane is retained in ER structures and this could have a buffering effect on ER morphology. Unlike the case of the Golgi, a variety of ER stress responses might be induced by the aberrant accumulation of secreted proteins in the ER by the inhibition of anterograde transport, and these responses might cause not only ER dysfunction but also the change in its morphology. Furthermore, accumulating evidence suggests that the communication between the early secretory organelles and plasma membrane exists. For example, signaling by growth factors (e.g. MAPK/ERK) at plasma membranes affects the early secretory pathway (anterograde transport) via the ERES (Farhan et al., 2010). Thus, it is important to investigate the overall balance of membrane trafficking between the relevant organelles, as well as the plasma membrane, to elucidate the changes in Golgi and ER morphology that occur during mitosis more fully. The quantitative analysis of membrane trafficking while the spatial configuration of cells is maintained will be of increasing significance. Therefore, our semi-intact cell assays will provide one suitable tool for studying the regulatory mechanisms of membrane trafficking, not only during mitosis, but also under other cellular conditions, for example, disease conditions.

9. References

Acharya, U.; Mallabiabarrena, A.; Acharya, J.K. & Malhotra. V. (1998). Signaling via mitogen-activated protein kinase kinase (MEK1) is required for Golgi fragmentation during mitosis. *Cell,* 92, pp.183–192.

Altan-Bonnet, N.; Sougrat, R.; Liu, W.;, Snapp, E.L.; Ward, T. & Lippincott-Schwartz, J. (2006). Golgi inheritance in mammalian cells is mediated through endoplasmic reticulum export activities. *Mol Biol Cell.*, 17(2), pp. 990-1005.

Bartz, R.; Sun, L.P.; Bisel, B.; Wei, J.H. & Seemann, J. (2008). Spatial separation of Golgi and ER during mitosis protects SREBP from unregulated activation *EMBO J.*, 27(7), pp. 948-55.

Bhakdi, S.; Tranum-Jensen, J. & Sziegoleit, A. (1985). Mechanism of membrane damage by streptolysin-O. *Infect Immun.*, 47(1), pp. 52-60.

Cole, N.B.; Smith, C.L.; Sciaky, N.; Terasaki, M.; Edidin, M. & Lippincott-Schwartz, J. (1996). Diffusional mobility of Golgi proteins in membranes of living cells. *Science*, 273, pp. 797–801.

Dreier, L. & Rapoport, T.A. (2000). In vitro formation of the endoplasmic reticulum occurs independently of microtubules by a controlled fusion reaction. *J Cell Biol.*,148(5), pp. 883-898.

Farhan, H.; Wendeler, M.W.; Mitrovic, S.; Fava, E.; Silberberg, Y.; Sharan, R.; Zerial, M. & Hauri, HP. (2010). MAPK signaling to the early secretory pathway revealed by kinase/phosphatase functional screening *J Cell Biol.*, 189(6), pp. 997-1011.

Feinstein, T.N. & Linstedt, A.D. (2007). Mitogen-activated protein kinase kinase 1-dependent Golgi unlinking occurs in G2 phase and promotes the G2/M cell cycle transition. *Mol Biol Cell.* 18(2), pp. 594-604.

Feinstein, T.N. & Linstedt, A.D. (2008). GRASP55 regulates Golgi ribbon formation. *Mol Biol Cell.*, 19(7), pp. 2696-2707.

Hetzer, M.; Meyer, H.H.; Walther, T.C.; Bilbao-Cortes, D.; Warren, G. & Mattaj, I.W. (2001). Distinct AAA-ATPase p97 complexes function in discrete steps of nuclear assembly. *Nat. Cell Biol.*, *3*, pp. 1086–1091.

Hughes, H. & Stephens, D.J. (2010). Sec16A defines the site for vesicle budding from the endoplasmic reticulum on exit from mitosis. *J Cell Sci.*, 123(Pt 23), pp. 4032-8.

Ikonen, E.; Tagaya, M.; Ullrich, O.; Montecucco, C. & Simons, K. (1995). Different requirements for NSF, SNAP, and Rab proteins in apical and basolateral transport in MDCK cells. *Cell.* 81, pp. 571–580.

Kano, F.; Takenaka, K.; Yamamoto, A.;Nagayama, K.; Nishida, E. & Murata, M. (2000a). MEK and Cdc2 kinase are sequentially required for Golgi disassembly in MDCK cells by the mitotic *Xenopus* extracts. *J. Cell Biol.*, pp. 357–368.

Kano, F.; Sako, Y.; Tagaya, M.; Yanagida, T. & Murata, M. (2000b). Reconstitution of brefeldin A-induced Golgi tubulation and fusion with the endoplasmic reticulum in semi-intact Chinese hamster ovary cells. *Mol. Biol. Cell*, 11, pp. 3073–3087.

Kano, F.; Tanaka, A.R.; Yamauchi, S.; Kondo, H. & Murata, M. (2004). Cdc2 kinase-dependent disassembly of endoplasmic reticulum (ER) exit sites inhibits ER-to-Golgi vesicular transport during mitosis. *Mol. Biol. Cell*. 15, pp. 4289-4298.

Kano, F.; Kondo, H.; Yamamoto, A.; Tanaka, A.R.; Hosokawa, N.; Nagata, K. & Murata, M. (2005). The maintenance of the ER network is regulated by p47, a cofactor of p97, through phosphorylation by cdc2 kinase. *Genes Cells*, 10, pp. 333–344.

Kano, F.; Kondo, H.; Yamamoto, A.; Kaneko, Y.; Uchiyama, K.; Hosokawa, N.; Nagata, K. & Murata, M. (2005). NSF/SNAPs and p97/p47/VCIP135 are sequentially required for cell cycle-dependent reformation of nthe ER network. *Genes Cells*, 10, pp. 989-999.

Kano,F.; Yamauchi,S.; Yoshida,Y.; Watanabe-Takahashi,M.; Nishikawa, K.; Nakamura, N. & Murata, M. (2009). Yip1A regulates the COPI-independent retrograde transport from the Golgi apparatus to the endoplasmic reticulum. *J. Cell Sci.*, 122, pp. 2218-2227.

Kondo, H.; Rabouille, C.; Newman, R.; Levine, T.P.; Pappin, D.; Freemont, P. & Warren, G. (1997). p47 is a cofactor for p97-mediated membrane fusion. *Nature*. 388(6637), pp. 75-8.

Lowe, M.; Rabouille, C.; Nakamura, N.; Watson, R.; Jackman, M.; Jamsa, E.; Rahman, D.; Pappin, D.J. & Warren, G. (1998). Cdc2 kinase directly phosphorylates the cis-Golgi

matrix protein GM130 and is required for Golgi fragmentation in mitosis. *Cell*. 94, pp. 783–793.

Lowe, M.; Gonatas, N.K. & Warren, G. (2000). The mitotic phosphorylation cycle of the cis-Golgi matrix protein GM130. *J Cell Biol*., 149(2), pp. 341-356.

Lu, L.; Ladinsky, M.S. & Kirchhausen, T. (2009). Cisternal organization of the endoplasmic reticulum during mitosis. *Mol Biol Cell*, 20(15), pp. 3471-3480.

Meyer, H.H.; Wang, Y. & Warren, G. (2002). Direct binding of ubiquitin conjugates by the mammalian p97 adaptor complexes, p47 and Ufd1-Npl4. *EMBO J*., 21(21), pp. 5645-5652.

Misteli, T. & Warren. G. (1995). A role for tubular networks and a COP I-independent pathway in the mitotic fragmentation of Golgi stacks in a cell-free system. *J Cell Biol*., pp. 1027-1039.

Preisinger, C.; Körner, R.; Wind, M.; Lehmann, W.D.; Kopajtich, R. & Barr, F.A. (2005). Plk1 docking to GRASP65 phosphorylated by Cdk1 suggests a mechanism for Golgi checkpoint signalling. *EMBO J.*, pp. 753-65.

Puhka, M.; Vihinen, H.; Joensuu, M. & Jokitalo, E. (2007). Endoplasmic reticulum remains continuous and undergoes sheet-to-tubule transformation during cell division in mammalian cells. *J Cell Biol*., 179(5), pp. 895-909.

Roy, L.; Bergeron, J.J.; Lavoie, C.; Hendriks, R.; Gushue, J.; Fazel, A.; Pelletier. A.; Morré, D.J.; Subramaniam, V.N.; Hong, W. & Paiement, J. (2000). Role of p97 and syntaxin 5 in the assembly of transitional endoplasmic reticulum. *Mol Biol Cell*, 11(8), pp. 2529-42.

Sengupta,D. & Linstedt, A.D. (2011). Control of Organelle Size: The Golgi Complex. *Annu. Rev. Cell Dev. Biol*., 27, pp. 5.1-5.21.

Shaul, Y.D. & Seger, R. (2006). ERK1c regulates Golgi fragmentation during mitosis. *J Cell Biol*., 172(6), pp. 885-897.

Tang, D.; Mar, K.; Warren, G. & Wang, Y. (2008). Molecular mechanism of mitotic Golgi disassembly and reassembly revealed by a defined reconstitution assay. *J Biol Chem*., 283(10), pp. 6085-6094.

Uchiyama, K.; Jokitalo, E.; Lindman, M.; Jackman, M.; Kano, F.; Murata, M.; Zhang, X. & Kondo, H. (2003). The localization and phosphorylation of p47 are important for Golgi disassembly-assembly during the cell cycle. *J Cell Biol*., 161, pp. 1067-1079.

Warren, G. (1993). Membrane partitioning during cell division. *Annu. Rev. Biochem.* 62, pp. 323–348.

Wei, J.H. & Seemann, J. (2009). Mitotic division of the mammalian Golgi apparatus. *Semin. Cell Dev. Biol*., 20(7), pp. 810-816.

Xie, S.; Wang, Q.; Ruan, Q.; Liu, T.; Jhanwar-Uniyal, M.; Guan, K. & Dai, W. (2004). MEK1-induced Golgi dynamics during cell cycle progression is partly mediated by Polo-like kinase-3. *Oncogene*, 23(21), pp. 3822-3829.

Yoshimura, S,; Yoshioka, K.; Barr, F.A.; Lowe, M.; Nakayama, K.; Ohkuma, S. & Nakamura, N. (2005). Convergence of cell cycle regulation and growth factor signals on GRASP65. *J Biol Chem*., 280(24), pp. 23048-23056.

Zaal, K.J.M.; Smith, C.L.; Polishchuk, R.S.; Altan, N.; Cole, N.B.; Ellenberg, J.; Hirschberg, K.; Presley, J.F.; Roberts, T.H.; Siggia, E.;Phair, A,D. & Lippincott-Schwartz, J. (1999). Golgi membranes are absorbed into and reemerge from the ER during mitosis. *Cell.* 99, pp. 589–601.

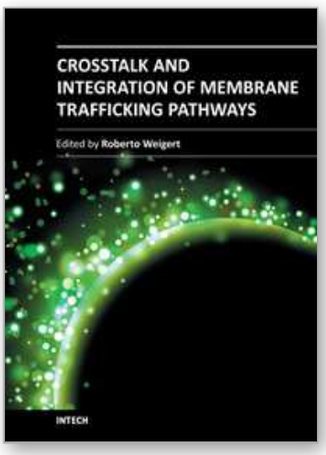

Crosstalk and Integration of Membrane Trafficking Pathways
Edited by Dr. Roberto Weigert

ISBN 978-953-51-0515-2
Hard cover, 246 pages
Publisher InTech
Published online 11, April, 2012
Published in print edition April, 2012

Membrane traffic is a broad field that studies the complex exchange of membranes that occurs inside the cell. Protein, lipids and other molecules traffic among intracellular organelles, and are delivered to, or transported from the cell surface by virtue of membranous carriers generally referred as "transport intermediates". These carriers have different shapes and sizes, and their biogenesis, modality of transport, and delivery to the final destination are regulated by a multitude of very complex molecular machineries. A concept that has clearly emerged in the last decade is that each membrane pathway does not represent a close system, but is fully integrated with all the other trafficking pathways. The aim of this book is to provide a general overview of the extent of this crosstalk.

How to reference
In order to correctly reference this scholarly work, feel free to copy and paste the following:

Masayuki Murata and Fumi Kano (2012). Semi-Intact Cell Systems - Application to the Analysis of Membrane Trafficking Between the Endoplasmic Reticulum and the Golgi Apparatus and of Cell Cycle-Dependent Changes in the Morphology of These Organelles, Crosstalk and Integration of Membrane Trafficking Pathways, Dr. Roberto Weigert (Ed.), ISBN: 978-953-51-0515-2, InTech, Available from: http://www.intechopen.com/books/crosstalk-and-integration-of-membrane-trafficking-pathways/semi-intact-cell-system-application-to-study-the-membrane-trafficking-between-the-endoplasmic-reticu

INTECH
open science | open minds

InTech Europe
University Campus STeP Ri
Slavka Krautzeka 83/A
51000 Rijeka, Croatia
Phone: +385 (51) 770 447
Fax: +385 (51) 686 166
www.intechopen.com

InTech China
Unit 405, Office Block, Hotel Equatorial Shanghai
No.65, Yan An Road (West), Shanghai, 200040, China
中国上海市延安西路65号上海国际贵都大饭店办公楼405单元
Phone: +86-21-62489820
Fax: +86-21-62489821

IntechOpen